Tautomerization of Phenols

Part III[1])

The Anthrone–Anthrol Equilibrium in Aqueous Solution

by **Beat Freiermuth**, **Bruno Hellrung**, **Stefan Peterli**, **Marie-France Schultz**, **David Wintgens**, and **Jakob Wirz***

Institut für Physikalische Chemie der Universität Basel, Klingelbergstrasse 80, CH-4056 Basel

Dedicated to Prof. *A. Jerry Kresge* on the occasion of his 75th birthday

The equilibrium between 10*H*-anthr-9-one and 9-anthrol favors the ketone, which ionizes as a carbon acid in aqueous base. Rates of equilibration were measured over the pH range 1–13 in aqueous solution (25°, ionic strength $I = 0.$ M). Five independent thermodynamic and kinetic parameters were determined by analysis of the pH-rate profile: the equilibrium constant of enolization, $pK_E = 2.17$, the ionization quotient of anthrol, $pQ_a^E = 7.84$, and the rate constants of enolization catalyzed by acid, $k_{H^+}^E = 2.2 \cdot 10^{-4}$ M^{-1} s^{-1}, base, $k_{HO^-}^E = 51.0$ M^{-1} s^{-1}, and water, $k_0^E = 1.21 \cdot 10^{-5}$ s^{-1}. Structure-reactivity relationships strongly support the view that pH-independent enolization of anthrone in water proceeds by rate-determining ionization of the C-acid.

Introduction. – Keto–enol tautomerism is a cornerstone of organic reactivity. Ninety years ago, *Meyer* [1] achieved the separation of solid 9-anthrol[2]) (**E**) from its more stable tautomer 10*H*-anthr-9-one[3]) (**K**). He also determined the equilibrium constant of enolization in EtOH solution, $K_E = [\mathbf{E}]/[\mathbf{K}] = 0.12$ [2]. Subsequent studies have dealt with the solvent [3–9] and temperature [10] dependence of the anthrone-anthrol equilibrium. Apolar solvents favor the ketone, hydrogen-bond acceptor solvents such as DMSO favor the enol. Kinetic data were reported for the enolization of anthrone induced by base catalysts in acetonitrile solution [6] and in apolar solvents [5]. The photophysical properties and photochemical reactions of anthrone were also investigated [11–18].

Over the last two decades, accurate equilibrium constants of enolization covering thirty orders of magnitude have been determined kinetically, *i.e.*, as ratios of enolization and ketonization rate constants in aqueous solution [19]. Few data are available for compounds with K_E close to unity [20, 21]. Such data are of interest for free-energy relationships and to determine the intrinsic barrier to proton transfer involving C-atoms. To fill the gap between ketones ($pK_E \approx 8$) and carboxylic acids or esters ($pK_E \approx 18$), which strongly favor the keto form, and phenol at the other extreme {pK_E(cyclohexa-2,4-dienone) $= -12.7$ [22]}, we have determined the kinetic and thermodynamic parameters of the anthrone-anthrol equilibrium in H_2O.

---

[1]) Part II: [22].

[2]) Trivial names: anthranol, anthrol; IUPAC nomenclature: anthracen-9-ol; *Chem. Abstr.:* 9-anthracenol.

[3]) *IUPAC* nomenclature: 9,10-dihydroanthracen-9-one; *Chem. Abstr.:* 9(10*H*)-anthracenone.

Keto–enol tautomerization is catalyzed by acids and bases. In aqueous solution, proton transfer through the solvent may result in an 'uncatalyzed' (pH-independent) reaction. The three reaction paths and the symbols used for the associated elementary rate and equilibrium constants are shown in the *Scheme*. The rate-determining step in each of these reactions involves proton transfer to or from C-atoms [19a]. Proton exchange between H_2O and the ketone or enol O-atom is fast on the time scale of proton-transfer reactions involving C-atoms. In other words, the equilibria for the dissociation of protonated anthrone, $\mathbf{K}^+ \rightleftharpoons \mathbf{K} + H^+$, and for the ionization of anthrol, $\mathbf{E} \rightleftharpoons \mathbf{E}^- + H^+$, may be regarded as fully established at all times, and the observed reaction rates reflect changes between the total ketone concentration, $[\mathbf{K}]_{tot} = [\mathbf{K}^+] + [\mathbf{K}]$, and the total enol concentration, $[\mathbf{E}]_{tot} = [\mathbf{E}^-] + [\mathbf{E}]$. The equilibrium and rate constants of the reactions shown in the *Scheme* are then fully defined by six independent parameters. All but the ionization constant of $\mathbf{K}^+$, $K_a^{K^+} = [\mathbf{K}][H^+]/[\mathbf{K}^+]$, were determined in this work. The results are in line with predictions from nonlinear free-energy relationships based on the *Marcus* theory for proton transfer [23], which indicates that the 'uncatalyzed' enolization of simple ketones and their α,β-unsaturated analogs in aqueous solution proceed by the same mechanism, namely rate-determining ionization of the C-acids.

Results. – *pH–Rate Profile.* Anthrone (**K**) is sparingly soluble in H_2O, $[\mathbf{K}]_{max} \approx 3 \cdot 10^{-6}$ M. The solubility increases to *ca.* $1 \cdot 10^{-4}$ M in aqueous base, where **K** ionizes to anthrolate ($\mathbf{E}^-$). Solutions of $\mathbf{E}^-$ were prepared and handled under exclusion of air to

Scheme

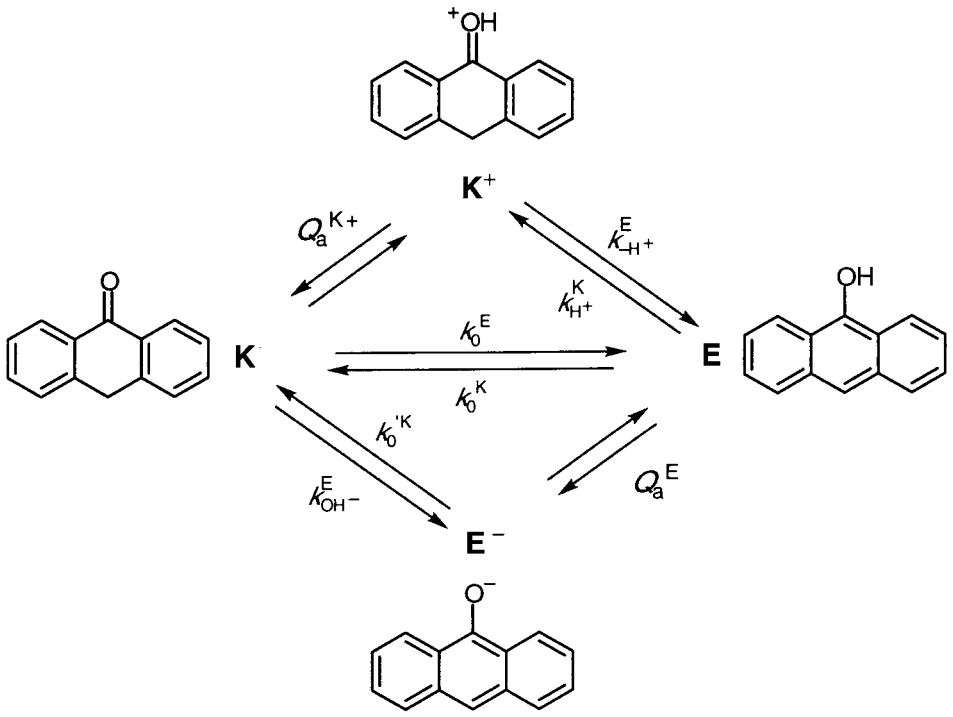

avoid oxidation to anthraquinone. For kinetic measurements, nonequilibrium concentrations of **K** or **E** must be generated on a time scale shorter than that of protomerization. Mixing neutral solutions of **K** with base in a stopped-flow apparatus generated solutions with excess **K** relative to the equilibrium concentration in aqueous base. Flash photolysis of **K** was the most convenient and accurate method to obtain reproducible excess concentrations of **E** in solutions of defined pH between 1 and 10. Photoenolization was previously observed in polar solvents [5, 9, 11–15], but photoreduction was the major reaction under the conditions used. Photoreduction does not compete in aqueous solutions of **K**, and photoenolization is fully reversible in the absence of oxygen. Presumably, photoenolization proceeds by ionization of excited **K** followed by rapid equilibration of $\mathbf{E}^-$ with **E**. Rates of approach to equilibrium were measured optically with a conventional spectrometer, a kinetic flash-photolysis setup, or a stopped-flow apparatus (*Exper. Part*). The ionic strength I was kept constant at 0.1 M by addition of NaCl.

The absorbance changes, $\Delta A_t = A_t - A_\infty$, associated with re-establishment of the equilibrium concentrations ($t = \infty$) accurately obeyed the first-order rate law at all pH values. The observed rate coefficient is the sum of the rate coefficients for the forward (enolization) and backward (ketonization) reaction, $k_{obs} = k^E + k^K$. The rate law for enolization is composed of three terms, the 'uncatalyzed', acid-catalyzed, and base-catalyzed reactions (*Scheme* and *Eqn. 1*).

$$-\mathrm{d}[\mathbf{K}]_{tot}/\mathrm{d}t = k_0^E[\mathbf{K}] + k_{-H^+}^E[\mathbf{K}^+] + k_{HO^-}^E[HO^-][\mathbf{K}] \quad (1)$$

Anthrone is a very weak base, and protonation of **K** is negligible in the pH range of 1–13 considered here (the acidity constant of protonated benzophenone was determined as $pK_a^{K^+} = -4.7$ [24]. Thus, $[\mathbf{K}] \gg [\mathbf{K}^+]$, $[\mathbf{K}]_{tot} \approx [\mathbf{K}]$, and $-\mathrm{d}[\mathbf{K}]_{tot}/\mathrm{d}t \approx -\mathrm{d}[\mathbf{K}]/\mathrm{d}t$. Replacing $[\mathbf{K}^+]$ by $[H^+][\mathbf{K}]/Q_a^{K^+}$ ($Q_a^{K^+}$ is the dissociation quotient of $\mathbf{K}^+$ at $I = 0.1$M), we obtain a pH-dependent first-order rate law, where the observed rate coefficient for enolization is a sum of the rate constants for the 'uncatalyzed', k_0^E, the acid-catalyzed, $k_{H^+}^E = k_{-H^+}^E/Q_a^{K^+}$, and the base-catalyzed reaction, $k_{HO^-}^E$ (*Eqn. 2*).

$$k^E = k_O^E + k_{H^+}^E[H^+] + k_{HO^-}^E[HO^-] \quad (2)$$

The concentration of hydroxyl ions may be replaced by $[HO^-] = K_w/[H^+]$, where $K_w = 1.59 \times 10^{-14}$ M is the ionization product of H_2O at ionic strength $I = 0$. M [25]. Similarly, the rate coefficient of ketonization is given by *Eqn. 3*, where Q_a^E is the ionization quotient of **E** at $I = 0$. M and the factor $[H^+]/(Q_a^E + [H^+])$ is equal to the mole fraction of $\mathbf{E}^-$ in equilibrium with **E**.

$$k^K = \{k_o^K + k_{H^+}^K[H^+] + k_0'^K\ Q_0^E/[H^+]\}\ [H^+]/(Q_a^E + [H^+]) \quad (3)$$

The ratio of the rate coefficients of enolization and ketonization must be equal to the enolization constant K_E for each reaction path. The resulting relations, $K_E = k_0^E/k_0^K = k_{H^+}^E/k_{H^+}^K = k_{HO^-}^E K_w/(k_0'^K Q_{a\ E})$, can be used to replace the rate constants k^K in *Eqn. 3*. Addition of *Eqns. 2* and *3* then gives *Eqn. 4* for the dependence of $k_{obs} = k^E + k^K$ on the proton concentration $[H^+]$ in wholly aqueous solution (*i.e.*, in the absence of buffers), which is a function of five parameters, k_0^E, $k_{H^+}^E$, $k_{HO^-}^E$, Q_a^E, and K_E.

$$k_{obs} = \{k_0^E + k_{H^+}^E[H^+] + k_{HO^-}^E K_w/[H^+]\}\{1 + [H^+]/[(Q_a^E + [H^+])K_E]\} \quad (4)$$

The results of the measurements are collected in *Tables 1* and *2*. The data are graphically represented as a pH–rate profile in *Fig. 1*. Rate constants determined in buffer solutions were extrapolated to zero buffer concentration (*vide infra*). The solid line in *Fig. 1* results from a nonlinear least-squares fit of *Eqn. 4* to the experimental data. The values of the five parameters determined by the fitting procedure are given in *Table 3*.

The acidity constant of **E** was independently determined by spectrophotometric titration of **E** on a time scale sufficient for equilibration of **E** with $\mathbf{E}^- + H^+$, but not for ionization of **K**. Reproducible excess concentrations of anthrol were generated by irradiation of anthrone with microsecond light flashes of constant energy. The initial absorbances changes ΔA_0 at 270 nm (*Fig. 2*) on $p[H^+]$ in the range of 4–10 follow a sigmoid titration curve (*Eqn. 5*), with inflection point equal to Q_a^E. The extinction coefficients ε_E and ε_{E^-} of anthrol and its anion refer to the monitoring wavelength of 270 nm, and $[\mathbf{E}]_{tot}$ is the total initial concentration of anthrol and its anion generated by flash photolysis.

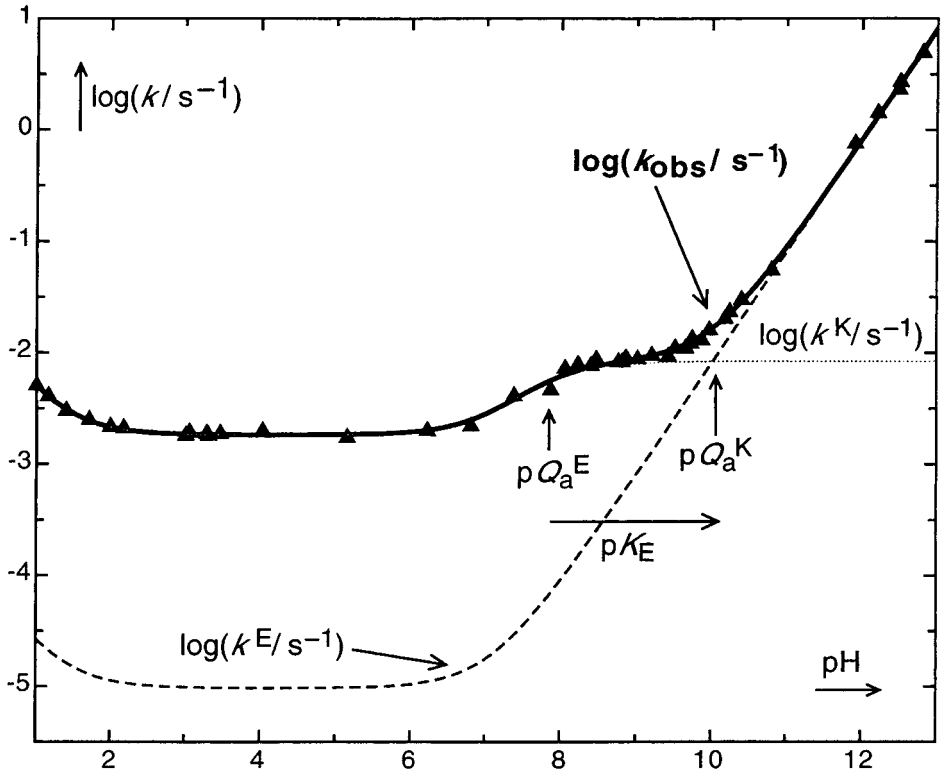

Fig. 1. *pH–Rate profile for the protomerization equilibrium* $\mathbf{E} \rightleftharpoons \mathbf{K}$. The solid line is the best fit of *Eqn. 4* to the data points. The dotted lines show the pH-dependences of the enolization rate constant k^E (---; *Eqn. 2*), and of the ketonization rate constant k^K (....; *Eqn. 3*), calculated with the parameters given in *Table 3*.

Table 1. *Kinetic Data for the Anthrone–Anthrol Equilibrium in Aqueous Solution* (25°, ionic strength $I = 0.10$M; rate constants are averages of 3–5 measurements)

Buffer	Method	k_{obs}/s^{-1}	$k_{buffer}/(M^{-1}\,s^{-1})$[h]	$[H^+]_{calc}/M$	$[H^+]_{meas}/M$
0.100M HCl	[a]	$(5.03 \pm 0.05) \cdot 10^{-3}$		$1.00 \cdot 10^{-1}$	
0.070M HCl	[a]	$(4.08 \pm 0.04) \cdot 10^{-3}$		$7.00 \cdot 10^{-2}$	
0.040M HCl	[a]	$(3.02 \pm 0.05) \cdot 10^{-3}$		$4.00 \cdot 10^{-2}$	
0.020M HCl	[a]	$(2.50 \pm 0.05) \cdot 10^{-3}$		$2.00 \cdot 10^{-2}$	
0.010M HCl	[a]	$(2.17 \pm 0.10) \cdot 10^{-3}$		$1.00 \cdot 10^{-2}$	$9.77 \cdot 10^{-3}$
0.001M HCl	[a]	$(1.81 \pm 0.02) \cdot 10^{-3}$		$1.00 \cdot 10^{-3}$	$9.55 \cdot 10^{-4}$
0.0005M HCl	[a]	$1.8 \cdot 10^{-3}$		$5.00 \cdot 10^{-4}$	$4.79 \cdot 10^{-4}$
$CH_2ClCOOH$/Na	[a]	$(2.1 \pm 0.1) \cdot 10^{-3}$[g]	$(1.69 \pm 0.05) \cdot 10^{-2}$	$6.61 \cdot 10^{-3}$	$6.27 \cdot 10^{-3}$
$CH_2ClCOOH$/Na	[a]	$(1.9 \pm 0.1) \cdot 10^{-3}$[g]	$(3.23 \pm 0.11) \cdot 10^{-2}$	$5.12 \cdot 10^{-4}$	$5.25 \cdot 10^{-4}$
HCOOH/Na	[a]	$(1.9 \pm 0.1) \cdot 10^{-3}$[g]	$(2.60 \pm 0.13) \cdot 10^{-2}$	$1.13 \cdot 10^{-3}$	$1.13 \cdot 10^{-3}$
HCOOH/Na	[a]	$(1.8 \pm 0.1) \cdot 10^{-3}$[g]	$(5.79 \pm 0.19) \cdot 10^{-2}$	$2.82 \cdot 10^{-4}$	$3.03 \cdot 10^{-4}$
HCOOH/Na	[a]	$(1.7 \pm 0.2) \cdot 10^{-3}$[g]	$(1.26 \pm 0.05) \cdot 10^{-1}$	$5.75 \cdot 10^{-5}$	$6.16 \cdot 10^{-5}$
MeCOOH/Na	[a]	$(1.8 \pm 0.1) \cdot 10^{-3}$[g]	$(7.75 \pm 0.20) \cdot 10^{-2}$	$1.04 \cdot 10^{-4}$	$9.70 \cdot 10^{-5}$
MeCOOH/Na	[a]	$(1.7 \pm 0.2) \cdot 10^{-3}$[g]	$(2.66 \pm 0.08) \cdot 10^{-1}$	$6.73 \cdot 10^{-6}$	$7.40 \cdot 10^{-6}$
NaH_2PO_4/Na_2HPO_4	[b][c]	$(2.1 \pm 0.3) \cdot 10^{-3}$[g]	1.06 ± 0.02	$6.64 \cdot 10^{-7}$	$6.02 \cdot 10^{-7}$
NaH_2PO_4/Na_2HPO_4	[b][c]	$(2.3 \pm 0.2) \cdot 10^{-3}$[g]	2.13 ± 0.03	$1.66 \cdot 10^{-7}$	$1.59 \cdot 10^{-7}$
NaH_2PO_4/Na_2HPO_4	[c]	$(3.6 \pm 0.3) \cdot 10^{-3}$[g]	3.52 ± 0.07	$4.15 \cdot 10^{-8}$	$4.36 \cdot 10^{-8}$
Tris/HCl	[b][c]	$(4.8 \pm 0.3) \cdot 10^{-3}$[g]	4.77 ± 0.05	$1.35 \cdot 10^{-8}$	$1.41 \cdot 10^{-8}$
Borax/HCl	[e]	$8.5 \cdot 10^{-3}$			$2.34 \cdot 10^{-9}$
Borax/HCl	[d]	$8.25 \cdot 10^{-3}$			$1.74 \cdot 10^{-9}$
Borax/HCl	[e]	$(8.20 \pm 0.3) \cdot 10^{-3}$			$1.55 \cdot 10^{-9}$
Borax/HCl	[d]	$(8.95 \pm 0.3) \cdot 10^{-3}$			$1.38 \cdot 10^{-9}$
Borax/HCl	[e]	$(8.72 \pm 0.2) \cdot 10^{-3}$			$9.77 \cdot 10^{-10}$
Borax/NaOH	[e]	$9.42 \cdot 10^{-3}$			$6.31 \cdot 10^{-10}$
Borax/NaOH	[e]	$9.22 \cdot 10^{-3}$			$3.80 \cdot 10^{-10}$
Borax/NaOH	[e]	$1.10 \cdot 10^{-2}$			$3.09 \cdot 10^{-10}$
Borax/NaOH	[e]	$1.10 \cdot 10^{-2}$			$2.24 \cdot 10^{-10}$
Borax/NaOH	[e]	$1.21 \cdot 10^{-2}$			$1.90 \cdot 10^{-10}$
Borax/NaOH	[e]	$1.33 \cdot 10^{-2}$			$1.82 \cdot 10^{-10}$
Borax/NaOH	[e]	$1.29 \cdot 10^{-2}$			$1.35 \cdot 10^{-10}$
Borax/NaOH	[e]	$(1.59 \pm 0.05) \cdot 10^{-2}$			$1.07 \cdot 10^{-10}$
Borax/NaOH	[e]	$(2.01 \pm 0.04) \cdot 10^{-2}$			$6.61 \cdot 10^{-11}$
Borax/NaOH	[e]	$(2.32 \pm 0.08) \cdot 10^{-2}$			$5.75 \cdot 10^{-11}$
Borax/NaOH	[e]	$(2.98 \pm 0.03) \cdot 10^{-2}$			$3.98 \cdot 10^{-11}$
0.001M NaOH	[f]	$5.50 \cdot 10^{-2}$		$1.59 \cdot 10^{-11}$	$1.51 \cdot 10^{-11}$
0.0115M NaOH	[f]	$(7.50 \pm 0.75) \cdot 10^{-1}$		$1.38 \cdot 10^{-12}$	
0.024M NaOH	[f]	1.41 ± 0.05		$6.63 \cdot 10^{-13}$	
0.049M NaOH	[f]	2.35 ± 0.10		$3.25 \cdot 10^{-13}$	
0.050M NaOH	[f]	2.69		$3.18 \cdot 10^{-13}$	
0.095M NaOH	[f]	4.93 ± 0.32		$1.67 \cdot 10^{-13}$	

[a]) Flash excitation, UV spectrophotometer, $\lambda_{obs} = 258$ nm. [b]) Flash excitation, spectrophotometer, $\lambda_{obs} = 269$ nm). [c]) Flash excitation, kinetic flash equipment, $\lambda_{obs} = 375$ nm (cut-off filter 345 nm). [d]) Flash excitation, spectrophotometer, $\lambda_{obs} = 269$ nm; 0.002M borax buffer, the observed rate constant was reduced by $7.9 \cdot 10^{-4}\,s^{-1}$ for buffer catalysis of borax. [e]) Mixing of borax buffer (0.002M and traces of NaOH) with an aqueous anthrone solution, spectrophotometer, $\lambda_{obs} = 269$ nm; the observed rate constant was reduced by $7.9 \cdot 10^{-4}\,s^{-1}$ for buffer catalysis by borax. [f]) Stopped-flow measurements, $\lambda_{obs} = 269$ nm. [g]) Intercepts determined by extrapolating the data given in *Table 2* to zero buffer concentration. [h]) Slopes determined by linear least-squares fitting of the data given in *Table 2*.

Table 2. *Catalysis by Buffers*[a])

$CH_2ClCOOH$, $pQ_a = 2.68$ ($I = 0.10$M)[b])				AcOH, $pQ_a = 4.57$ ($I = 0.10$M)[c])				*Tris*/HCl, $pK_{a,c} = 8.12$ ($I = 0.10$M)[d])			
pH 2.19, $x_{HA} = 0.756$		pH 3.28, $x_{HA} = 0.201$		pH 4.02, $x_{HA} = 0.780$		pH 5.13, $x_{HA} = 0.216$		pH 7.82, $x_{HA} = 0.666$		pH 7.82, $x_{HA} = 0.666$	
[bu]/M	k_{obs}/s^{-1}	[bu]/M	k_{obs}/s^{-1}	[bu]/M	k_{obs}/s^{-1}	[bu]/M	k_{obs}/s^{-1}	[bu]/M	k_{obs}/s^{-1}	[bu]/M	k_{obs}/s^{-1}
$2.5 \cdot 10^{-2}$	$2.53 \cdot 10^{-3}$	$2.5 \cdot 10^{-2}$	$2.67 \cdot 10^{-3}$			$1.0 \cdot 10^{-2}$	$4.55 \cdot 10^{-3}$	$1.5 \cdot 10^{-3}$	$1.17 \cdot 10^{-2}$	$4.5 \cdot 10^{-2}$	$2.18 \cdot 10^{-1}$
$7.5 \cdot 10^{-2}$	$3.41 \cdot 10^{-3}$	$7.5 \cdot 10^{-2}$	$4.36 \cdot 10^{-3}$	$2.0 \cdot 10^{-2}$	$3.35 \cdot 10^{-3}$	$2.0 \cdot 10^{-2}$	$6.60 \cdot 10^{-3}$	$3.0 \cdot 10^{-3}$	$1.86 \cdot 10^{-2}$	$6.0 \cdot 10^{-2}$	$3.00 \cdot 10^{-1}$
$1.0 \cdot 10^{-1}$	$3.75 \cdot 10^{-3}$			$4.0 \cdot 10^{-2}$	$5.02 \cdot 10^{-3}$	$4.0 \cdot 10^{-2}$	$1.22 \cdot 10^{-2}$	$4.5 \cdot 10^{-3}$	$2.55 \cdot 10^{-2}$	$7.5 \cdot 10^{-2}$	$3.51 \cdot 10^{-1}$
$1.25 \cdot 10^{-1}$	$4.24 \cdot 10^{-3}$	$1.25 \cdot 10^{-1}$	$5.85 \cdot 10^{-3}$	$6.0 \cdot 10^{-2}$	$6.61 \cdot 10^{-3}$	$6.0 \cdot 10^{-2}$	$1.85 \cdot 10^{-2}$	$7.5 \cdot 10^{-3}$	$4.03 \cdot 10^{-2}$		
				$8.0 \cdot 10^{-2}$	$8.08 \cdot 10^{-3}$	$8.0 \cdot 10^{-2}$	$2.30 \cdot 10^{-2}$	$7.5 \cdot 10^{-3}$	$4.18 \cdot 10^{-2}$		
				$1.0 \cdot 10^{-1}$	$9.37 \cdot 10^{-3}$	$1.0 \cdot 10^{-1}$	$2.85 \cdot 10^{-2}$	$3.0 \cdot 10^{-2}$	$1.50 \cdot 10^{-1}$		
$k_{HA} = (1.0 \pm 0.1) \cdot 10^{-2}$ M^{-1} s^{-1} $k_{A^-} = (3.8 \pm 0.2) \cdot 10^{-2}$ M^{-1} s^{-1}				$k_{HA} \leq 4 \cdot 10^{-3}$ M^{-1} s^{-1} $k_{A^-} = (3.4 \pm 0.2) \cdot 10^{-1}$ M^{-1} s^{-1}				$k_{A^-} \approx 14$ M^{-1} s^{-1}			

HCOOH, $pQ_a = 3.55$ ($I = 0.10$M)[e])						NaH_2PO_4, $pQ_a = 6.78$ ($I = 0.10$M)[f])					
pH 2.94, $x_{HA} = 0.803$		pH 3.52, $x_{HA} = 0.517$		pH 4.21, $x_{HA} = 0.18$		pH 6.22, $x_{HA} = 0.784$		pH 6.80, $x_{HA} = 0.489$		pH 7.36, $x_{HA} = 0.208$	
[bu]/M	k_{obs}/s^{-1}	[bu]/M	k_{obs}/s^{-1}	[bu]/M	k_{obs}/s^{-1}	[bu]/M	k_{obs}/s^{-1}	[bu]/M	k_{obs}/s^{-1}	[bu]/M	k_{obs}/s^{-1}
$2.0 \cdot 10^{-2}$	$2.37 \cdot 10^{-3}$	$3.0 \cdot 10^{-2}$	$3.52 \cdot 10^{-3}$	$2.0 \cdot 10^{-2}$	$4.25 \cdot 10^{-3}$	$2.22 \cdot 10^{-3}$	$4.55 \cdot 10^{-3}$	$2.0 \cdot 10^{-3}$	$6.58 \cdot 10^{-3}$	$2.0 \cdot 10^{-3}$	$1.10 \cdot 10^{-2}$
$4.0 \cdot 10^{-2}$	$3.01 \cdot 10^{-3}$	$4.0 \cdot 10^{-2}$	$4.13 \cdot 10^{-3}$	$4.0 \cdot 10^{-2}$	$6.63 \cdot 10^{-3}$	$4.44 \cdot 10^{-3}$	$6.78 \cdot 10^{-3}$	$4.0 \cdot 10^{-3}$	$1.06 \cdot 10^{-2}$	$4.0 \cdot 10^{-3}$	$1.81 \cdot 10^{-2}$
$6.0 \cdot 10^{-2}$	$3.53 \cdot 10^{-3}$	$6.0 \cdot 10^{-2}$	$5.4 \cdot 10^{-3}$	$6.0 \cdot 10^{-2}$	$9.58 \cdot 10^{-3}$	$6.66 \cdot 10^{-3}$	$9.18 \cdot 10^{-3}$	$6.0 \cdot 10^{-3}$	$1.50 \cdot 10^{-2}$	$6.0 \cdot 10^{-3}$	$2.62 \cdot 10^{-2}$
$8.0 \cdot 10^{-2}$	$3.94 \cdot 10^{-3}$	$8.0 \cdot 10^{-2}$	$6.52 \cdot 10^{-3}$	$8.0 \cdot 10^{-2}$	$1.17 \cdot 10^{-2}$	$6.66 \cdot 10^{-3}$	$9.80 \cdot 10^{-3}$	$8.0 \cdot 10^{-3}$	$1.96 \cdot 10^{-2}$	$8.0 \cdot 10^{-3}$	$3.28 \cdot 10^{-2}$
$1.0 \cdot 10^{-1}$	$4.43 \cdot 10^{-3}$	$1.0 \cdot 10^{-1}$	$7.44 \cdot 10^{-3}$			$1.33 \cdot 10^{-2}$	$1.59 \cdot 10^{-2}$	$1.0 \cdot 10^{-2}$	$2.45 \cdot 10^{-2}$	$5.0 \cdot 10^{-3}$	$2.11 \cdot 10^{-2}$
						$2.66 \cdot 10^{-2}$	$3.16 \cdot 10^{-2}$	$2.0 \cdot 10^{-2}$	$4.70 \cdot 10^{-2}$	$1.0 \cdot 10^{-2}$	$4.01 \cdot 10^{-2}$
						$4.00 \cdot 10^{-2}$	$4.60 \cdot 10^{-2}$	$3.0 \cdot 10^{-2}$	$6.47 \cdot 10^{-2}$	$2.0 \cdot 10^{-2}$	$7.60 \cdot 10^{-2}$
						$5.33 \cdot 10^{-2}$	$5.60 \cdot 10^{-2}$	$4.0 \cdot 10^{-2}$	$8.56 \cdot 10^{-2}$	$3.0 \cdot 10^{-2}$	$1.02 \cdot 10^{-1}$
						$6.66 \cdot 10^{-2}$	$7.15 \cdot 10^{-2}$	$5.0 \cdot 10^{-2}$	$1.07 \cdot 10^{-1}$	$4.0 \cdot 10^{-2}$	$1.47 \cdot 10^{-1}$
$k_{HA} \leq 5 \cdot 10^{-3}$ M^{-1} s^{-1}, $k_{A^-} = (1.4 \pm 0.1) \cdot 10^{-1}$ M^{-1} s^{-1}						$k_{A^-} = 4.2 \pm 0.3$ M^{-1} s^{-1}					

[a]) Buffer concentrations: $[bu] = [HA] + [A^-]$, ionic strength $I = 0.1$M. Ionization quotients Q_a of the buffers were calculated from thermodynamic ionization constants given in the literature and activity coefficients for $I = 0.1$M recommended by *Bates* [25]. [b]) [26]. [c]) [27]. [d]) [28]. [e]) [29]. [f]) [30].

Table 3. *Summary of Kinetic and Thermodynamic Parameters* (25°; equilibrium constants are concentration quotients for $I = 0.1$M)

Reaction	Constant[a])	Value
$\mathbf{K} \rightarrow \mathbf{E}$	k_0^E	$(1.21 \pm 0.15) \cdot 10^{-5}$ s^{-1}
$\mathbf{K} \rightarrow \mathbf{E}$ (acid cat.)	$k_{H^+}^E$	$(2.2 \pm 0.3) \cdot 10^{-4}$ M^{-1} s^{-1}
$\mathbf{K}^+ \rightarrow \mathbf{E} + H^+$	$k_{-H^+}^E = k_{H^+}^E Q_a^{K^+}$[b])	≈ 10 s^{-1}[b])
$\mathbf{K} + HO^- \rightarrow \mathbf{E}^- + H_2O$	$k_{HO^-}^E$	51.0 ± 1.0 M^{-1} s^{-1}
$\mathbf{E} \rightarrow \mathbf{K}$	$k_0^K = k_0^E / K_E$	$(1.8 \pm 0.3) \cdot 10^{-3}$ s^{-1}
$\mathbf{E} + H^+ \rightarrow \mathbf{K}^+$	$k_{H^+}^K = k_{H^+}^E / K_E$	$(3.2 \pm 0.6) \cdot 10^{-2}$ M^{-1} s^{-1}
$\mathbf{E}^- + H_2O \rightarrow \mathbf{K} + HO^-$	$k_0^K = k_{HO^-}^E K_w / (K_E\, Q_a^E)$[c])	$(8.3 \pm 0.3) \cdot 10^{-3}$ M^{-1} s^{-1}
$\mathbf{E}^- + H^+ \rightarrow \mathbf{K}$	$k_{H^+}^K = k_0^K / Q_a^E$	$(1.24 \pm 0.24) \cdot 10^5$ M^{-1} s^{-1}
$\mathbf{E} \rightleftharpoons \mathbf{E}^- + H^+$	pQ_a^E	7.84 ± 0.04
$\mathbf{K} \rightleftharpoons \mathbf{E}$	pK_E	2.17 ± 0.05
$\mathbf{K} \rightleftharpoons \mathbf{E}^- + H^+$	$pQ_a^K = pK_E + pQ_a^E$	10.01 ± 0.06

[a]) Where an equation is given, it was used to calculate the constant from the experimentally determined quantities on the right-hand side of the expression. [b]) $pQ_a^{K^+}$ of protonated anthrone assumed to be equal to the dissociation constant of protonated benzophenone, $pK_a^{K^+} = -4.7$ [24]. [c]) Ionization product of water: $K_w(I = 0.1\text{M}) = 1.59 \cdot 10^{-14}$ M^2 [25].

$$\Delta A_0 = \frac{\varepsilon_E\,[H^+] + \varepsilon_{E^-}\,Q_a^E}{[H^+] + Q_a^E}\,[\mathbf{E}]_{tot} \tag{5}$$

Nonlinear least-squares fitting of *Eqn. 5* to the data points ΔA_0 gave $pQ_a^E = (7.83 \pm 0.06)$. This value is equal, within the limits of error, to that obtained from analysis of the pH–rate profile, $pQ_a^E = 7.84 \pm 0.06$. The average of the two measurements is $pQ_a^E = 7.84 \pm 0.04$.

The acidity constant of protonated anthrone $\mathbf{K}^+$ cannot be determined from the present data, because $pQ_a^{K^+}$ lies well below the pH range of 1–13 considered here. The rate constant $k_{-H^+}^E = k_{H^+}\,Q_a^{K^+}$ (*Scheme*) may be estimated as $k_{-H^+}^E \approx 10$ s^{-1} by assuming that the dissociation quotient of $\mathbf{K}^+$, $Q_a^{K^+}$, is equal to the acidity constant of protonated benzophenone, $pK_a = -4.7$ [24].

Buffer Catalysis. The observed rate coefficients (*Table 2*) increased linearly with increasing buffer concentration at constant buffer ratio (*i.e.*, constant pH; *Eqn. 6*).

$$k_{obs} = k_0^* + k_{buffer}\,[\text{buffer}] \tag{6}$$

Extrapolation to zero buffer concentration gave the intercepts k_0^* of *Eqn. 6* (*Table 1*), which were used in the least-squares fit of *Eqn. 4*. The slopes k_{buffer} were linearly related to the mole fractions of the acidic and basic buffer components (*Eqn. 7*), and the catalytic coefficients k_{HA} and k_{A^-} for the acidic and basic components of the buffer were obtained from the intercepts for $x_{HA} = 0$ and $x_{HA} = 1$[4]). General acid catalysis was detected only for the most acidic buffer, $CH_2ClCOOH$. The results are given in *Table 2*.

$$k_{buffer} = x_{HA}\,k_{HA} + (1 - x_{HA})k_{A^-}, \text{ where } x_{HA} = [HA]/([HA] + [A^-]) \tag{7}$$

[4]) The coefficients k_{HA} and k_{A^-} were determined by nonlinear fitting to $\log\{k_{buffer}/(\text{M}^{-1}\,\text{s}^{-1})\}$ in order to account for the fact that the standard errors of the slopes k_{buffer} are proportional to their absolute values.

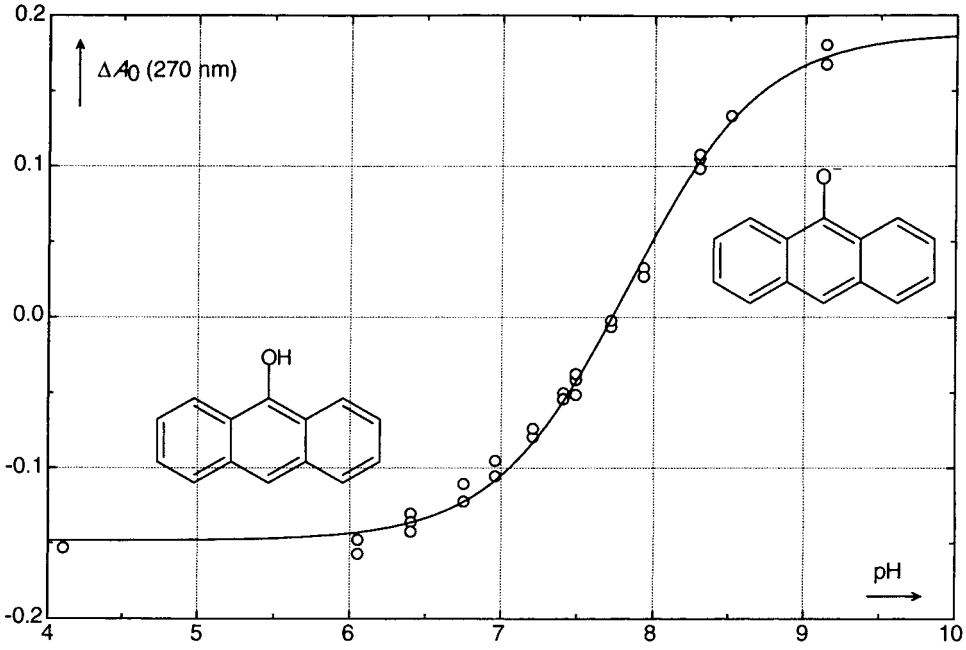

Fig. 2. *Titration curve for the ionization of* **E** *determined by flash photolysis.* The data points are initial absorbances A_0 at 270 nm immediately after the flash. The solid line is the best fit of *Eqn. 5* to the data points.

Electronic Spectra. The electronic spectra of anthrone (**K**), anthrol (**E**), and anthrolate ($\mathbf{E}^-$) are shown in *Fig. 3*. All solutions were prepared and handled in the dark under Ar. Solutions of **K** were prepared by dissolving weighed amounts of the recrystallized sample in 5 ml MeCN and diluting to a total volume of 100 ml with 0.01N HCl. A small peak at 256 nm indicated the presence of *ca.* 6% of **E**, somewhat in excess of the amount expected from the equilibrium constant for enolization. This may be due to the presence of **E** in the recrystallized sample or to some photoenolization by adventitious light. The spectrum shown for 'pure' **K** ($\lambda_{max} = 271$, $\log(\varepsilon/[\text{M}^{-1}\,\text{cm}^{-1}]) = 4.27 \pm 0.02$) was generated by subtracting 6% of the spectrum of **E**, determined as described below, from the observed spectrum. The resulting spectrum was normalized by multiplication with a factor of 1.06. The spectrum of $\mathbf{E}^-$ ($\lambda_{max} = 268$, $\log(\varepsilon/[\text{M}^{-1}\,\text{cm}^{-1}]) = 4.95 \pm 0.03$) was obtained by the addition of a degassed MeCN solution of **K** to 0. M aqueous NaOH. A solution strongly enriched in **E** ($\lambda_{max} = 256$, $\log(\varepsilon/[\text{M}^{-1}\,\text{cm}^{-1}]) = 5.03 \pm 0.05$) was generated by irradiation of a solution of **K** in 0.0 M HCl with a high-pressure Hg arc lamp through an optical filter transmitting from 250 to 400 nm (*Schott UG 5*). Under these conditions, the photoenolization was clean and fully reversible in the dark. The photostationary state contained *ca.* 25% **K**, as indicated by a shoulder at 271 nm. The spectrum of 'pure' **E** shown in *Fig. 3* was obtained by deduction of 25% of the spectrum of **K** from that of the photostationary mixture and normalization.

Preparation of Anthrol (**E**). *Meyer*'s method for isolation of solid anthrol (**E**) [1], addition of $\mathbf{E}^-$ in 5% aqueous base to 5% aqueous H_2SO_4, is difficult to reproduce. More reliable procedures have been described [3][31]. The pH–rate profile (*Fig. 1*)

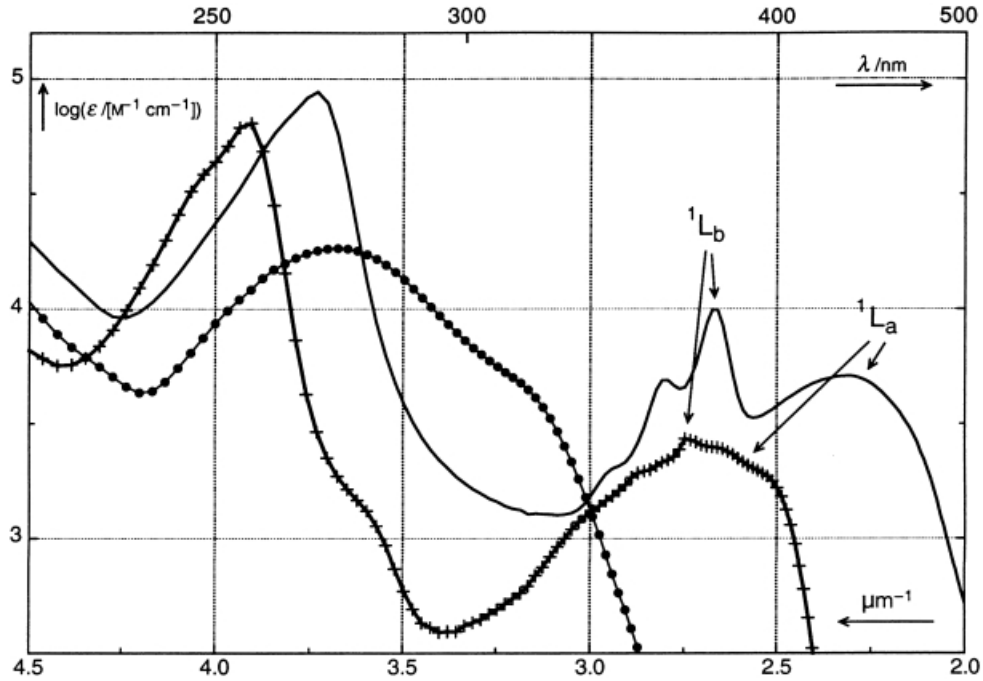

Fig. 3. *Absorption spectra of anthrone* (**K**; –●–●–), *anthrol* (**E**; – + – + –), and *anthrolate* ($\mathbf{E}^-$; ——) *in aqueous solution*, *25°*. For clarity of presentation, the spectrum of **E** was shifted downward by 0.5 log units.

indicates that reketonization of **E** is slowest in the pH range of 2–6. Thus, a precipitate of **E** essentially free of **K** was obtained simply by rapid addition of a slight excess of cold aqueous 0. M HCl to a saturated, cold, deoxygenated solution of $\mathbf{E}^-$ in 0. M aqueous NaOH containing 0.0 M AcONa. However, the precipitate reketonized upon drying.

Calculations for **K** and **E** were performed with the GAUSSIAN 98 [32] package of programs based on the B3LYP density functional theory with the standard 6-31G(d) basis set. Geometries were fully optimized without symmetry restrictions, and frequency calculations were done at the energy minimum. B3LYP is a combination of *Becke*'s three-parameter exchange functional [33] with a slightly modified *Lee–Yang–Parr* [34] correlation functional. The results are given in *Table 4*. The resulting minimum-energy structures of both compounds were planar (except for the two CH_2 H-atoms of anthrone). The standard free-energy change calculated for the enolization of anthrone corresponds to a calculated (gas phase) equilibrium constant of $pK_E = 6.4$.

Discussion. – Anthrone (**K**) is the predominant tautomer in aqueous solution at pH < 10. It ionizes as a carbon acid forming anthrolate ($\mathbf{E}^-$) in aqueous base. Excess concentrations of **E** at pH < 10 were generated by photoenolization, and excess concentrations of **K** at pH > 10 by rapid mixing of neutral solutions with base. Relaxation to the equilibrium concentrations obeyed a first-order rate law at all pH values. The dependence of the observed rate coefficients k_{obs} (*Table 1*) on proton

Table 4. *Density Functional Calculations for Anthrol and Anthrone*

	Anthrone (**K**)	Anthrol (**E**)	
SCF energy/h	−614.759556		−614.744258
Zero-point energy/h	0.199053		0.198128
$\{H^\circ(298\ K) - H^\circ(0\ K)\}$/h	0.011621		0.012001
$S^\circ(298\ K)/(J\ K^{-1}\ mol^{-1})$	429		437
$\Delta_{K\to E}H^\circ(g, 298\ K)/(kJ\ mol^{-1})$		38.7	
$\Delta_{K\to E}G^\circ(g, 298\ K)/(kJ\ mol^{-1})$		36.3	

concentrations (*Eqn. 4*) is graphically represented as a pH–rate profile (*Fig. 1*). The kinetic and thermodynamic parameters resulting from a least-squares fit of *Eqn. 4* to the experimental data are given in *Table 3*. Enolization of anthrone followed by ionization of anthrol amounts to ionization of anthrone as a carbon acid. Hence, the ionization quotient of anthrone, Q_a^K, is equal to the product $K_E\,Q_a^E$, that is $pQ_a^K = pK_E + pQ_a^E = 10.01 \pm 0.06$.

The rate profile is best interpreted by considering the rate coefficients for enolization, k^E, and ketonization, k^K, separately. The functions k^E and k^K shown in *Fig. 1* were calculated with *Eqn. 2* for k^E and with *Eqn. 3* for k^K on the basis of the parameters given in *Table 3*. Up to pH 9, $k_{obs} = k^K + k^E$ is close to k^K, *i.e.*, $k^K \gg k^E$, reflecting the higher stability of **K** in neutral and acidic aqueous solutions. The rate of deprotonation of **K** increases with increasing concentration of OH^-, and k^E exceeds k^K at $pH > pQ_a^K = 10.01$. Thus, k^E is the dominant term of k_{obs} at $pH > 10$.

The rate profile exhibits downward curvature at $pH \approx 8$, which is attributed to preequilibrium ionization of **E** to $\mathbf{E}^- + H^+$, and three regions of upward curvature ($pH \approx 2, 7, 10$), all of which indicate a change in the dominant reaction mechanism with changing acid concentration. Therefore, four different reactions contribute to the rate profile. The portion rising with a slope of -1 at $pH < 2$ reflects the acid-catalyzed pathway of the *Scheme*, $\mathbf{E} + H^+ \to \mathbf{K}^+ \rightleftharpoons \mathbf{K} + H^+$, for which k_{obs} is proportional to $[H^+]$. Going to higher pH, we encounter the first region of upward curvature at pH 2, and a pH-independent, 'uncatalyzed' reaction dominates in the pH range 3–6. The mechanism of this reaction will be discussed below. The rise of k_{obs} at pH 7 is due to the onset of ketonization of **E** by pre-equilibrium ionization followed by rate-determining C-atom protonation of $\mathbf{E}^-$, $\mathbf{E} \rightleftharpoons \mathbf{E}^- + H^+ \to \mathbf{K}$. This reaction rate saturates at $pH \approx pQ_a^E = 7.84$, where ionization of **E** becomes quantitative. Finally, k_{obs} rises again as the base-catalyzed enolization of **K** becomes dominating at $pH > 10$.

Catalysis by General Acids and Bases. Analysis of the buffer dilution plots gave well-defined coefficients, k_{A^-}, for the acceleration of the observed rate constant by the base components, A^-. General acid catalysis was detected for only the most acidic buffer used, $CH_2ClCOOH/Na$. The logarithms of the coefficients k_{A^-} (five points; *Table 2*) were linearly related to the pQ_a^{HA} values of the buffers, and the slope of this plot gave a *Brønsted* coefficient $\beta = 0.47 \pm 0.02$ and an intercept of -2.59 ± 0.10.

$$\log(k_{A^-}/M^{-1}\ s^{-1}) = \text{const} + \beta pQ_a^{HA} \tag{8}$$

The rate-determining step in the general-base catalyzed enolization is the C-atom deprotonation of **K** by the basic buffer component, $\mathbf{K} + A^- \to \mathbf{E}^- + HA$. The reverse

reaction, C-atom protonation of the enolate by the general acid, $\mathbf{E}^- + HA \rightarrow \mathbf{K} + A^-$, is rate-determining for the ketonization of **E**, but is preceded by a rapid pre-equilibrium $\mathbf{E} + A^- \rightleftharpoons \mathbf{E}^- + HA$. The observed overall coefficient for general base catalysis, $k_{A^-} = k^E_{A^-} + k^K_{A^-}$ is dominated by the term for ketonization, $k^K_{A^-} = k'^K_{AH} Q^E_a / Q^{HA}_a$. At the midpoint $pQ^{HA}_a = 5.1$ of the buffers used here, the standard free-energy change for the rate-determining step for ketonization, $\mathbf{E}^- + HA \rightarrow \mathbf{K} + A^-$, is moderately exergonic, $\Delta_r G^\circ = 2.3\ RT(pQ^{HA}_a - pQ^K_a) = -28$ kJ mol^{-1}. Thus, a *Brønsted* coefficient β slightly below 0.5 is reasonable.

The shape of the kinetic rate profile and the observation of both general acid and general base catalysis are consistent with the generally accepted mechanism for the protomerization of simple ketones (*Scheme*). The enolization constant of anthrone, $pK_E = 2.17$, and the acidity constant of 9-anthrol, $pK^E_a = 7.84$, obtained here agree well with the values of 2.1 and 7.9, respectively, that *Harcourt* and *More O'Ferrall* reported as unpublished results [35].

Mechanism of the pH-Independent Reaction. The 'uncatalyzed' term is barely recognizable at the bottom of the pH–rate profiles for the enolization of simple ketones [36], but dominates that for ketonization of cyclohexa-2,4-dienone to phenol, which is independent of pH in the range of 3–10 [22]. In the intermediate case of anthrol (*Fig. 1*), the pH-independent term is still quite important, dominating the overall rate in the range pH = 3–6. Apparently, the pH-independent term of *Eqn. 4* becomes more important relative to the terms for acid and base catalysis as the keto–enol equilibrium shifts towards the enol form. We now show that this is in line with *Marcus* theory for proton transfer [23].

Several mechanisms may be considered for the pH-independent kinetic term of keto–enol protomerization [36], namely stepwise proton transfer through the solvent with H_2O acting as base (*Eqn. 9*) or as an acid (*Eqn. 10*), as well as a concerted mechanism involving a H_2O molecule as a proton relay. Intramolecular 1,3-H shifts may be ruled out on the basis of their prohibitive calculated activation energies. Intramolecular 1,5-H shifts may, however, be competitive for α,β-unsaturated ketones with (*Z*)-configuration, such as (*Z*)-pent-3-en-2-one. All of these mechanisms result in a pH-independent rate law and are, therefore, kinetically indistinguishable.

$$\mathbf{E} + H_2O \rightleftharpoons \mathbf{E}^- + H_3O^+ \rightarrow \mathbf{K} + H_2O \quad (9)$$

$$\mathbf{E} + H_2O \rightarrow \mathbf{K}^+HO^- \rightleftharpoons \mathbf{K} + H_2O \quad (10)$$

The stepwise mechanism shown in *Eqn. 10* was ruled out for simple ketones [36] by estimating the reactivity of H_2O as a general acid on the basis of the *Brønsted* equation. The same argument can be applied in the present case. Using *Eqn. 11* with the coefficient of general acid catalysis for $CH_2ClCOOH$ ($k_{HA} = 1.0 \cdot 10^{-2}$ M^{-1} s^{-1}, *Table 2*), $\alpha \approx 0.5$, $pQ^{HA}_a = 2.7$, and $pQ^{H_2O}_a = 15.5$, the estimated rate for C-protonation of **E** by H_2O as a general acid (first step of *Eqn. 10*) is $k_{H_2O} \approx 4 \cdot 10^{-9}$ M^{-1} s^{-1}, which corresponds to $k^K_0 = 55\text{M} \cdot k_{H_2O} \approx 2 \cdot 10^{-7}$ s^{-1}, 4 orders of magnitude less than the experimental value (*Table 3*). The *Brønsted* coefficient α may be somewhat lower than 0.5, because the reaction considered is endergonic by 108 kJ mol^{-1}. However, α would have to be lowered to 0.2 to bring the estimate near to the experimental value, which is unrealistic.

In fact, α must exceed 0.34 to accommodate the fact that the coefficient for general acid catalysis by formic acid was too small to be detected, $k_{HA} \leq 5 \cdot 10^{-3}$ M^{-1} s^{-1} (*Table 2*).

$$\log(k_{H_2O}) = \log(k_{HA}) + \alpha(pQ_a^{HA} - pQ_a^{H_2O}) \quad (11)$$

Structure–reactivity relationships for a series of simple ketones have been shown to be inconsistent with a concerted mechanism through a bridging water molecule [36]. In the case of anthrone, concerted proton transfer would require at least two bridging H_2O molecules, which renders such a mechanism even less likely. *We are thus left with two-step proton transfer through water* (*Eqn. 9*), *as the most plausible mechanism for the pH-independent reaction*. According to this mechanism, the rate coefficient k_0^K decomposes to $k'^K_{H^+} Q_a^E$. The rate constant for the second, rate-determining step of *Eqn. 9* is then calculated as $k'^K_{H^+} = (1.24 \pm 0.24) \cdot 10^5$ M^{-1} s^{-1}. The rate coefficient for the uncatalyzed term, $k_0 = 55$M k_{H_2O}, may be estimated from the *Brønsted* equation for solvent water acting as a general base (*Eqn. 8*, $pQ_a^{H_3O^+} = -1.74$). The result, $\log(k_0/s^{-1}) = -1.7 \pm 0.4$, is within an order of magnitude of the experimental value, $\log(k_0^K/s^{-1}) = -2.7 \pm 0.1$.

Further, strong support for this mechanism comes from the fact that free-energy relationships for the rate constants $k'^K_{H^+}$, determined as above from observed values of k_0^K, and of k'^K_0, which cover a range of 20 orders of magnitude, obey a systematic, nonlinear relationship that is well reproduced by the *Marcus* expression [23] for proton transfer. A fit of the *Marcus* expression to data points for many keto–enol equilibria (including that of anthrone) gave an intrinsic barrier of $\Delta G_0^{\neq} = 57 \pm 2$ kJ mol^{-1} [19a,b]. Ketonization rate constants $k'^K_{H^+}$, which are responsible for the pH-independent term in the rate profiles, approach the diffusion-controlled limit for highly exergonic reactions (enols of ketones with low enolization constants such as simple ketones, carboxylic acids and esters, $pK_E \gtrsim 8$), and hardly increase with the driving force of the reaction ($\alpha \ll 0.5$). The rate constants $k_{H^+}^K$ and k'^K_0 that give rise to the competing terms for acid and base catalysis are much slower, and gain from a large driving force for ketonization ($\alpha \approx 0.5$). This explains why the uncatalyzed term is negligible in ketones, carboxylic acids, and esters, but is the dominant term for compounds with higher enolization constants.

Experimental Part

Materials. Anthrone (yellow powder; *Fluka*) was recrystallized twice from benzene/petroleum ether 3:1 to remove traces (*ca.* 0.5%) of anthraquinone, giving colorless needles, m.p. 155.0–156.5°, which were dried under vacuum and stored in the absence of air and light.

Buffers (phosphate (NaH_2PO_4/Na_2HPO_4, pH 6.0–7.5), *Tris* (tris(hydroxymethyl)aminomethane/HCl, pH 7.6–8.6), borax ($Na_2B_4O_7 \cdot 10\ H_2O$/NaOH, pH 9.1–9.2)) were of best available commercial grades and were used as received. Stock solns. of the buffer acid or its conjugate sodium salt were adjusted to the required proton concentration by addition of either NaOH or HCl (*Titrisol*, *Merck*) and to ionic strength of $I = 0.10$M by the addition of NaCl. The pH of the solns. was measured with a glass electrode that had been calibrated with NBS buffers, pH 1.68, 4.01, 6.86, or 9.18 (25°). The pH readings thus obtained should be equal to $-\log[H^+]$ within 0.02 log units [37], and this was found to be the case when proton concentrations $[H^+]$ were calculated from the buffer composition (*Table 2*). All solns. were prepared under Ar with doubly distilled H_2O.

Procedures. The solubility of anthrone in H_2O is poor (*ca.* $3 \cdot 10^{-6}$ M), and the solns. are sensitive to light and air (autoxidation to anthraquinone [38–40]). Degassed solns. of up to $1 \cdot 10^{-5}$ M anthrone were stable in the dark with 2% MeCN as a cosolvent. These solns. were prepared by dissolving a weighed sample of anthrone in a small

amount of MeCN and diluting to the desired volume with degassed, doubly distilled H_2O. All kinetic experiments were done in thermostatted cells that were kept at $25.0 \pm 0.5°$. Slow kinetics ($k_{obs} < 10^{-2}\ s^{-1}$) were measured on a conventional double-beam optical spectrophotometer *Perkin-Elmer Lambda-9* that was equipped with thermostatted cell holders and operated in the time-drive mode. The best wavelengths for observation were determined by measuring transient spectra with a *Hewlett-Packard 8452A* diode-array spectrophotometer (integration time 1 s).

For faster kinetic measurements, a conventional, home-built kinetics flash photolysis system with an electric discharge flash lamp (max. 1000 J electrical energy, ≤ 30 μs half-width) was used. Stopped-flow measurements were performed on a *Union Giken RA 401* instrument equipped with a thermostatted sample compartment and a 2-mm quartz cell. Appropriate filters were used to exclude photolysis of the sample by the monitoring light.

Phototitration Experiments. Buffer solns. (phosphate, *Tris*, borax) with equal concentrations of anthrone (*ca.* $1 \cdot 10^{-5}$ M) and ionic strength $I = 0.10$M were prepared, degassed, and thermostatted at $25 \pm 0.5°$. An excess concentration of anthrol(ate) was generated by irradiation of anthrone with a flash of constant energy. The initial change of absorbance at 270 nm, ΔA_0, induced by the flash was monitored on the conventional flash-photolysis equipment. In experiments with *Tris* buffers, photoreduction competed with photoenolization. Therefore, the ΔA_0 values obtained with *Tris* buffers were discarded.

Kinetic Experiments. Measurements in the pH range 11 – 13 were made by rapid mixing of equal volumes of degassed, aqueous solns. of anthrone and aq. NaOH in a stopped-flow apparatus. The formation of anthrolate was followed at 269 nm. In the pH range 9.5 – 10.5 a different procedure was used. Ar-flushed solns. of anthrone in H_2O with the appropriate buffer were filled into two separate, thermostatted sample compartments connected to a 1-cm quartz cuvette. After rapid mixing, formation of the anthrolate was followed at 269 nm. A small amount of borax buffer (0.002 – 0.005M) was added to control pH, which was checked with a glass electrode after the experiments. The observed rate constants were corrected using the measured catalytic constant $k_{A^-} = 0.37\ M^{-1}\ s^{-1}$ for the basic component of the borax buffer, which was determined from buffer dilution plots at three buffer ratios. The required corrections were below 10% at the low buffer concentrations used.

For measurements at pH < 9.5, excess **E** was generated by a light flash or by brief UV irradiation with a medium-pressure Hg arc lamp. For measurement in the pH range of 7 – 9, where substantial amounts of $\mathbf{E}^-$ were produced by irradiation, solns. were thoroughly degassed by three freeze-pump-thaw cycles in order to avoid oxidation to anthraquinone. These measurements, in 10-cm quartz cells, were best done at wavelength 370 to 375 nm. Samples were protected from UV light by shielding the monitoring light beam with an optical cut-off filter, $\lambda > 350$ nm, placed before the sample compartment.

This work was supported by the *Swiss National Science Foundation*.

REFERENCES

[1] K. H. Meyer, *Liebigs Ann. Chem.* **1911**, *379*, 37.
[2] K. H. Meyer, A. Sander, *Liebigs Ann. Chem.* **1913**, *396*, 133.
[3] K. Nukada, Y. Bansho, *Bull. Chem. Soc. Jpn.* **1953**, *26*, 454; Y. Bansho, K. Nukada, *Bull. Chem. Soc. Jpn.* **1960**, *33*, 579.
[4] G. Löber, *Acta Chim. Hung.* **1964**, *40*, 9; G. Löber, *Z. wiss. Photogr. Photophys. Photochem.* **1965**, *59*, 20.
[5] H. Baba, T. Takemura, *Tetrahedron* **1968**, *24*, 4779; T. Takemura, H. Baba, *Tetrahedron* **1968**, *24*, 5311.
[6] F. M. Menger, R. F. Williams, *J. Org. Chem.* **1974**, *39*, 2131.
[7] P. Beak, F. S. Fry Jr., J. Lee, F. Steele, *J. Am. Chem. Soc.* **1976**, *98*, 171.
[8] S. G. Mills, P. Beak, *J. Org. Chem.* **1985**, *50*, 1216.
[9] K. Almdal, H. Eggert, O. Hammerich, *Acta Chem. Scand.*, *Ser. B* **1986**, *40*, 230.
[10] H. Sterk, *Monatsh. Chem.* **1969**, *100*, 916.
[11] G. Löber, *Z. Phys. Chem. N. F. (Frankfurt)* **1967**, *54*, 73.
[12] N. Kanamaru, S. Nagakura, *J. Am. Chem. Soc.* **1968**, *90*, 6905.
[13] G. Gauglitz, *Z. Phys. Chem. N. F. (Wiesbaden)* **1974**, *88*, 193.
[14] J. C. Scaiano, C. W. B. Lee, Y. L. Chow, G. E. Buono-Core, *J. Photochem.* **1982**, *20*, 327.
[15] R. W. Redmond, J. C. Scaiano, *J. Photochem. Photobiol., A: Chem.* **1989**, *49*, 203.
[16] J. C. Netto-Ferreira, D. Weir, J. C. Scaiano, *J. Photochem. Photobiol.*, *A: Chem.* **1989**, *48*, 345.

[17] P. F. McGarry, C. E. Doubleday Jr., C.-H. Wu, H. A. Staab, N. J. Turro, *J. Photochem. Photobiol. A: Chem.* **1994**, *77*, 109; D. E. Damschen, C. D. Merritt, D. L. Perry, G. W. Scott, L. D. Talley, *J. Phys. Chem.* **1978**, *82*, 2268; G. W. Scott, L. D. Talley, *Chem. Phys. Lett.* **1977**, *52*, 431; T. Kobayashi, S. Nagakura, *Chem. Phys. Lett.* **1976**, *43*, 429.
[18] T. Fujii, S. Mishima, N. Tanaka, O. Kawauchi, K. Kodaira, H. Nishikiori, Y. Kawai, *Res. Chem. Interm.* **1977**, *23*, 829.
[19] a) J. Wirz, *Chem. in unserer Zeit* **1998**, *32*, 311; b) J. Wirz, *Pure Appl. Chem.* **1998**, *70*, 2221; c) J. R. Keefe and A. J. Kresge in 'The Chemistry of Enols', Ed. Z. Rappoport, Wiley, New York, 1990, Chapt. 7; J. Toullec, *ibid.*, pp. 323–398.
[20] M. Eigen, *Angew. Chem.* **1963**, *75*, 489.
[21] Y. Chiang, A. J. Kresge, E. T. Krogh, *J. Am. Chem. Soc.* **1988**, *110*, 2600.
[22] M. Capponi, I. G. Gut, B. Hellrung, G. Persy, J. Wirz, *Can. J. Chem.* **1999**, *77*, 605.
[23] A. O. Cohen, R. A. Marcus, *J. Phys. Chem.* **1968**, *72*, 4249.
[24] A. Bagno, V. Lucchini, G. Scorrano, *J. Phys. Chem.* **1991**, *95*, 345.
[25] R. G. Bates, 'Determination of pH. Theory and Practice', Wiley, New York, 1973.
[26] D. J. G. Ives, J. H. Pryor, *J. Chem. Soc.* **1955**, 2104.
[27] H. S. Harned, R. W. Ehlers, *J. Am. Chem. Soc.* **1933**, *55*, 652.
[28] R. G. Bates, H. B. Hetzer, *J. Phys. Chem.* **1961**, *63*, 667.
[29] H. S. Harned, N. D. Embree, *J. Am. Chem. Soc.* **1934**, *56*, 1042; M. Kilpatrick, R. D. Eanes, *J. Am. Chem. Soc.* **1953**, *75*, 586.
[30] A. K. Grzybowski, *J. Phys. Chem.* **1958**, *62*, 555.
[31] H. L. J. Bäckström, H. A. Beatty, *J. Phys. Chem.* **1931**, *35*, 2530.
[32] Gaussian 98, Revision A.7, M. J. Frisch, G. W. Trucks, H. B. Schlegel, G. E. Scuseria, M. A. Robb, J. R. Cheeseman, V. G. Zakrzewski, J. A. Montgomery Jr., R. E. Stratmann, J. C. Burant, S. Dapprich, J. M. Millam, A. D. Daniels, K. N. Kudin, M. C. Strain, O. Farkas, J. Tomasi, V. Barone, M. Cossi, R. Cammi, B. Mennucci, C. Pomelli, C. Adamo, S. Clifford, J. Ochterski, G. A. Petersson, P. Y. Ayala, Q. Cui, K. Morokuma, D. K. Malick, A. D. Rabuck, K. Raghavachari, J. B. Foresman, J. Cioslowski, J. V. Ortiz, A. G. Baboul, B. B. Stefanov, G. Liu, A. Liashenko, P. Piskorz, I. Komaromi, R. Gomperts, R. L. Martin, D. J. Fox, T. Keith, M. A. Al-Laham, C. Y. Peng, A. Nanayakkara, C. Gonzalez, M. Challacombe, P. M. W. Gill, B. Johnson, W. Chen, M. W. Wong, J. L. Andres, C. Gonzalez, M. Head-Gordon, E. S. Replogle, J. A. Pople, *Gaussian, Inc.*, Pittsburgh PA, 1998.
[33] A. D. Becke, *J. Chem. Phys.* **1993**, *98*, 5648.
[34] a) C. Lee, W. Yang, R. G. Parr, *Phys. Rev. B* **1988**, *37*, 785; b) P. J. Stephens, F. J. Devlin, C. F. Chabalowski, M. J. Frisch, *J. Phys. Chem.* **1994**, *98*, 11623.
[35] M. P. Harcourt, R. A. More O'Ferrall, *J. Chem. Soc., Perkin Trans. 2* **1995**, 1415.
[36] Y. Chiang, A. J. Kresge, J. A. Santabella, J. Wirz, *J. Am. Chem. Soc.* **1988**, *110*, 5506.
[37] H. Sigel, A. D. Zuberbühler, O. Yamauchi, *Anal. Chim. Acta* **1991**, *255*, 63.
[38] Y. Ogata, Y. Kosugi, K. Nate, *Tetrahedron* **1971**, *27*, 2705.
[39] H. Mauser, G. Gauglitz, *Chem. Ber.* **1973**, *106*, 1985.
[40] N. Filipescu, E. Avram, K. D. Welk, *J. Org. Chem.* **1977**, *42*, 507.

Received June 29, 2001